

Direct evidence for dynamic magma supply fossilized in the lower oceanic crust of the Troodos ophiolite

Roi Granot, Meir Abelson, Hagai Ron, Matthew W. Lusk, Amotz Agnon

▶ **To cite this version:**

Roi Granot, Meir Abelson, Hagai Ron, Matthew W. Lusk, Amotz Agnon. Direct evidence for dynamic magma supply fossilized in the lower oceanic crust of the Troodos ophiolite. Geophysical Research Letters, 2011, 38, 10.1029/2011GL048220 . insu-03606458

HAL Id: insu-03606458

https://insu.hal.science/insu-03606458

Submitted on 12 Mar 2022

HAL is a multi-disciplinary open access archive for the deposit and dissemination of scientific research documents, whether they are published or not. The documents may come from teaching and research institutions in France or abroad, or from public or private research centers.

L'archive ouverte pluridisciplinaire **HAL**, est destinée au dépôt et à la diffusion de documents scientifiques de niveau recherche, publiés ou non, émanant des établissements d'enseignement et de recherche français ou étrangers, des laboratoires publics ou privés.

Copyright

Direct evidence for dynamic magma supply fossilized in the lower oceanic crust of the Troodos ophiolite

Roi Granot,[1,2] Meir Abelson,[3] Hagai Ron,[4] Matthew W. Lusk,[5] and Amotz Agnon[4]

Received 20 May 2011; revised 21 July 2011; accepted 21 July 2011; published 24 August 2011.

[1] Temporal and spatial variabilities of mantle upwelling and melt supply in mid-ocean ridges (MORs) have long been documented. Such variabilities span a range of scales and have a profound effect on the structure as well as the composition of the oceanic crust. Previous seismic and gravity studies have suggested that the lower oceanic crust plays a major role in accommodating these changes in melt supply. Here we report the first direct evidence for a sharp transition from coherent sub-horizontal to near vertical magma flows frozen in the lower oceanic crust of the Troodos ophiolite at the segment edge near a fossil ridge-transform intersection. We constrain the preferred petrofabric lineation directions at 13 gabbroic sites using anisotropy of magnetic susceptibility (AMS) verified by electron backscatter diffraction. Pre-emplacement accretion-related rotations were corrected using magnetic remanence directions. We identify two provinces of nearly uniform susceptibility directions (principal axes) and attribute them to two magmatic episodes. A more focused mantle upwelling and melting episode near the segment midpoint may have resulted in lower crustal lateral magma flows along the fossil segment-edge, whereas uniform mantle upwelling and melt supply along the entire axis may have resulted in vertical magma flows at the segment-edge. Overall, our data verify the vital role of the lower oceanic crust in accommodating changes in mantle upwelling and melt supply beneath MORs. **Citation:** Granot, R., M. Abelson, H. Ron, M. W. Lusk, and A. Agnon (2011), Direct evidence for dynamic magma supply fossilized in the lower oceanic crust of the Troodos ophiolite, *Geophys. Res. Lett.*, *38*, L16311, doi:10.1029/2011GL048220.

1. Introduction

[2] Accumulating observations from the seafloor and ophiolites suggest that transient mantle upwelling with intermittent magmatic activity best describe the accretion of the oceanic crust along MORs [*Bonatti et al.*, 2003; *Perfit et al.*, 1994]. States of enhanced versus reduced magmatic activity alternate on timescales of ~100 kyr [*Canales et al.*, 2000; *Perfit et al.*, 1994] to a few million of years [*Bonatti et al.*, 2003; *Tucholke et al.*, 1997]. The spatial and temporal evolution of magmatic activity affect axial thermal structure [*Searle and Escartin*, 2004], development of detachment faults [*Olive et al.*, 2010], geometry of spreading segments [*Abelson and Agnon*, 2001; *Abelson et al.*, 2002; *Toomey et al.*, 2007], as well as composition of the oceanic crust [*Rubin et al.*, 2009]. This study addresses the yet poorly resolved question of how magma flows in the lower oceanic crust accommodate different modes of mantle upwelling and melting conditions beneath spreading axes.

[3] At slow-spreading axes, gravity, seismic tomography, and morphological studies suggest that the centers of spreading segments are commonly the sites of focused mantle upwelling and magma supply [*Dunn et al.*, 2005; *Magde et al.*, 2000; *Tucholke and Lin*, 1994]. Seismic refraction studies indicate that thickening of seismic layer 3 at these segment mid-points result in the thickest crust there [*Muller et al.*, 1999; *Tolstoy et al.*, 1993]. In this scenario, melt is channeled from the segment mid-point toward the magma-starved segment edges by lateral transport of magma within the lower gabbroic crust [*Abelson et al.*, 2001; *Hosford et al.*, 2001] and upper crustal sheeted dikes [*Magde et al.*, 2000]. Alternatively, segment-scale mantle upwelling and melt production have been inferred to exist in fast spreading axes [e.g., *Kent et al.*, 1993] and in certain magma-rich slow spreading segments [*Tucholke et al.*, 1997]. Under the latter magmatic conditions, melt is expected to rise mostly vertically from the mantle along the entire length of spreading segments. These two modes of melting conditions are expected to be most distinctive at the segment-edge where vertical melt transport in the lower crust may reflects uniform mantle upwelling and melt supply along spreading segment, while lateral transport of melt indicates focused mantle upwelling, and suggests melt supply below the segment mid-point.

[4] The oceanic crust exposed on the island of Cyprus (Troodos ophiolite) provides a unique opportunity to directly examine the temporal evolution of magma flow directions in the lower oceanic crust at a fossil segment-edge. Here we report magnetic fabric and petrofabric results from the gabbroic rocks of the Troodos ophiolite, sampled along a spreading-parallel profile located near the fossilized segment-edge. Our AMS results are clustered into two adjacent regions of nearly uniform fabric directions (sub-horizontal and near-vertical), implying an abrupt switch between two prevailing modes of magma flows.

2. Tectonic Setting

[5] The oceanic crust of the Troodos ophiolite formed along the Neotethyan spreading system during the late Cretaceous (92.1 Ma [*Mukasa and Ludden*, 1987]), in a supra-subduction zone setting. The uplift of the ophiolite had a minimal impact on the internal structure and composition of the crust [*Robertson and Xenophontos*, 1993], making the

[1]Institut de Physique du Globe de Paris, Sorbonne Paris Cité, Université Paris Diderot, Paris, France.
[2]Now at Department of Geological and Environmental Sciences, Ben-Gurion University of the Negev, Beer-Sheva, Israel.
[3]Geological Survey of Israel, Jerusalem, Israel.
[4]Institute of Earth Sciences, Hebrew University of Jerusalem, Jerusalem, Israel.
[5]Department of Geology and Geophysics, University of Wyoming, Laramie, Wyoming, USA.

Copyright 2011 by the American Geophysical Union.
0094-8276/11/2011GL048220

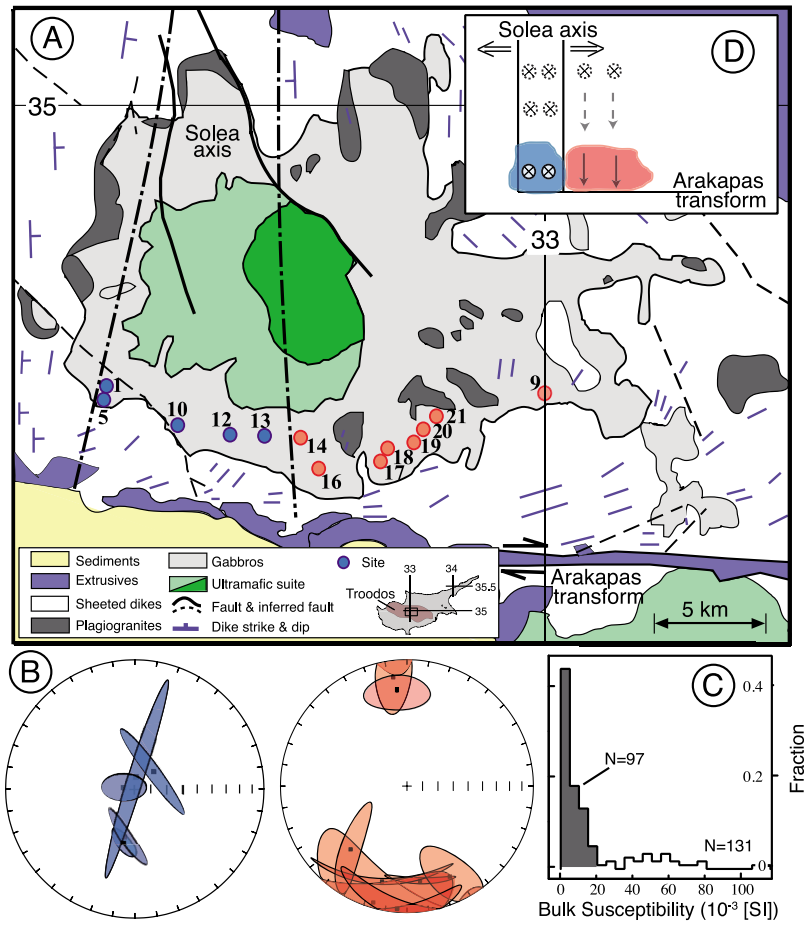


Figure 1. Anisotropy of magnetic susceptibility (AMS) data. (a) Site locations. The two colors for the sampled sites correspond to the two groups of directions for the major axes of AMS shown in Figure 1b. Dashed thick lines indicate the location of the paleospreading Solea axis. (b) Equal area, lower hemisphere projection of the mean bootstrapped K_1 AMS results. These directions are tilt-corrected (Figure S1). (c) Histogram showing the fraction of gabbroic specimens per bulk magnetic susceptibility ($(k_1 + k_2 + k_3)/3$). Shaded area marks the fraction used in our analysis. (d) Schematic diagram summarizing the spatial and temporal evolution of magmatic activity within the lower crust. Dashed lines represent speculated magma flow directions north of the studied area.

Troodos ophiolite an ideal location to study crustal accretion processes. Field mapping and geochemical studies [*Malpas*, 1990; *Schouten and Kelemen*, 2002] indicate that the lower parts of the Troodos spreading axis were composed from a set of discrete, short-lived magma bodies.

[6] Extensive structural observations lay out the tectonic context for our study. The center of the ophiolite exposes the fossil intersection of a N-S spreading axis, the Solea graben, and the E-W Arakapas dextral transform fault [*MacLeod et al.*, 1990] (Figure 1). The location of the Solea graben was originally constrained by the orientation of normal faults, opposing tilt of sheeted dikes, and rotated blocks of lava flow [*Hurst et al.*, 1994]. Paleomagnetic study of the gabbroic suite [*Granot et al.*, 2006] confirmed the location of the suspected paleospreading Solea axis and showed a clockwise rotation of remanence directions in the inside corner north of the Arakapas Transform fault (Figure S1 in the auxiliary material), similar to the rotations shown for the overlying sheeted dikes [*Allerton*, 1989; *Bonhommet et al.*, 1988], pillow lavas and hydrothermal sediments (umbers) [*Morris et al.*, 1990].[1]

3. Sampling

[7] We sampled 17 gabbro and olivine-gabbro sites, all located within the upper kilometer below the sheeted dike-gabbro contact (Figure 1). These sites are located at the continuation of the extinct spreading axis of the Solea graben and aligned along a flow-line direction giving the opportunity to study crustal accretion processes in a time sequence. We sampled the macroscopically isotropic gabbros, which lack any visible structural markers (foliations, lineations, horizontal or vertical layering, and veins). In site we have randomly sampled five to seven oriented cores over some 5 to 15 meters of exposure to unravel

[1]Auxiliary materials are available in the HTML. doi:10.1029/2011GL048220.

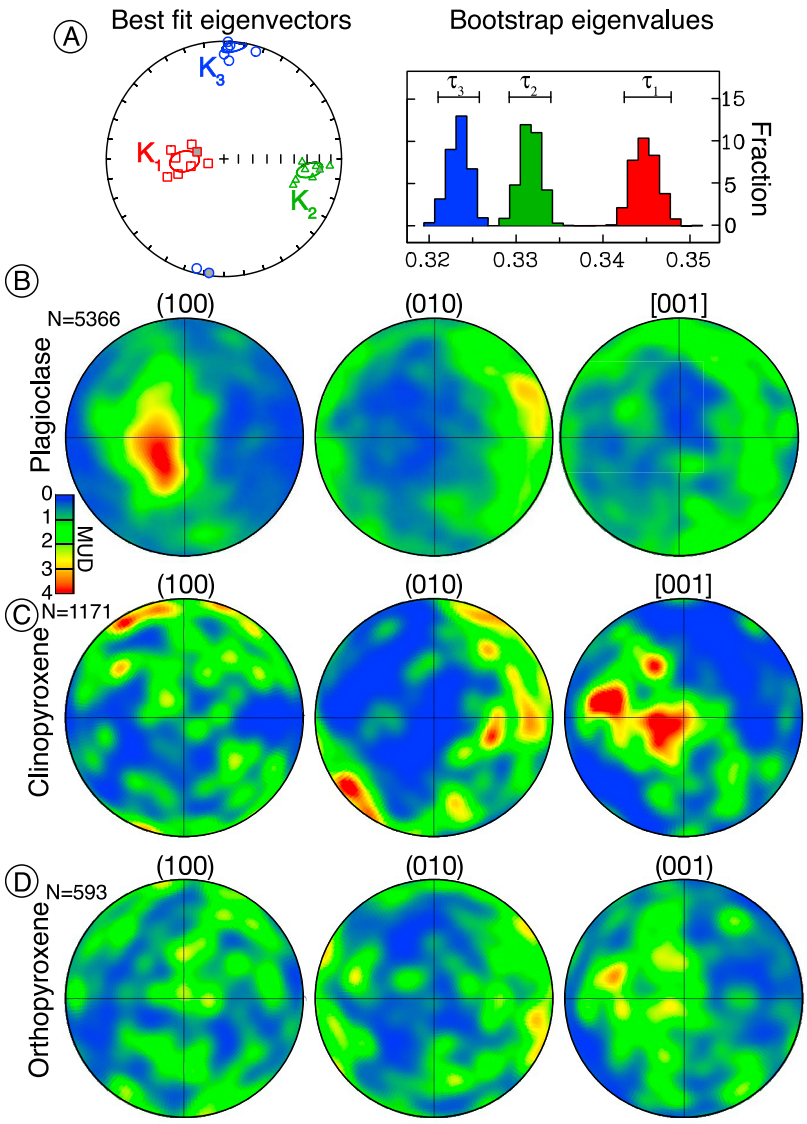


Figure 2. Comparison between anisotropy of magnetic susceptibility (AMS) and silicate crystallographic fabrics, projected in geographical coordinates. (a) The AMS data show (left) the eigenvector directions and (right) the associated eigenvalues of all specimens from site T12. Gray filled symbols highlight the results of specimen T12-1. Red squares are eigenvectors K_1 associated with maximum eigenvalues (τ_1). Green triangles are eigenvectors K_2 associated with intermediate eigenvalues (τ_2), and blue circles are eigenvectors K_3 associated with minimum eigenvalues (τ_3). 95% confidence bounds are calculated using the bootstrap method of *Tauxe et al.* [1998]. Electron backscattered diffraction (EBSD) data for specimen T12-1. (b) Plagioclase, (c) Clinopyroxene, and (d) Orthopyroxene are lower hemisphere pole projections contoured with a 15° half-width. Color scale corresponds to multiples of uniform distribution (MUD). N is number of grains, where each measurement corresponds to an individual grain. Methods are described in the Data Repository.

the dominant trend of the silicate fabric. Paleomagnetic data from the studied sites have been published elsewhere [*Granot et al.*, 2006, 2007].

4. Magma Flow Direction

[8] The low field AMS directions were measured with a Sapphire Instruments SI-2 susceptibility meter in a 6 orientation scheme. We applied bootstrap analysis [*Constable and Tauxe*, 1990] to obtain the three principal axes (directions of eigenvectors, $k_1 > k_2 > k_3$) and the associated 95% confidence bounds that best describe the AMS second-order tensor for each one of the sites. To avoid biased petrofabric interpretation due to magnetite distributions unrelated to magma flow (such as secondary magnetite formed by hydrothermal activity), we consider only specimens with low bulk susceptibility ($<20 \times 10^{-3}$ SI, Figure 1c). We are left with a total of 97 out of 131 specimens located in 15 successful sites (each featuring more than 4 specimens). The calculated tensors are mostly characterized by triaxial to prolate ellipsoid shapes (13 out of the remaining 15 sites). As discussed further later in the text, for our tectonic interpretation we only consider the major eigenvector (k_1) and therefore we exclude from further consideration the two spherical to oblate

sites. All the successful AMS data are presented in Figure S2 and Table S1 of the auxiliary material. The sampled gabbros have significant degrees of anisotropy [*Jelinek*, 1981], ranging between 2% to 24% with an average of 6%.

[9] The link between the preferred orientation of the AMS tensors and the petrofabric is not obvious and requires additional constraints before further interpretation can be made. Previous investigations of gabbros from the Troodos ophiolite showed a qualitative agreement between AMS directions and alignment of silicate fabrics observed in oriented thin sections [*Abelson et al.*, 2001, 2002]. These studies attributed AMS to distribution anisotropy [*Hargraves et al.*, 1991], in which late crystallization of titanomagnetite from the residual liquid is spatially governed by the pre-existing lattice preferred orientation of the silicate fabric. Since neither high-temperature recrystallization nor mechanical twining were observed, *Abelson et al.* [2001, 2002] concluded that AMS data for the Troodos gabbros reflect the last stages of magma flow, before the solidification of the residual melt, rather than solid-state deformation. Plagioclase crystallographic fabrics of the gabbroic sections of the Oman ophiolite [*Yaouancq and MacLeod*, 2000], the Hess Deep [*MacLeod et al.*, 1996], and continental layered intrusions [e.g., *Gee et al.*, 2004] show a good correspondence to the AMS directions, further supporting the link between the orientation of gabbroic AMS and the silicate fabric. To verify this link for the Troodos gabbros, we estimate the preferred crystallographic orientation of the silicate fabric for one test specimen (T12-1) using electron backscatter diffraction (EBSD, details are given in the auxiliary material) and compare these data with the AMS data from the entire site (T12).

[10] Our EBSD analysis reveals a distinct crystallographic lineation in plagioclase that sub-parallels the orientation of the major AMS axes (Figure 2). The plagioclase lattice preferred orientation (LPO) reveals a (100) maximum, dipping westwards at ~70°, similar to the weaker clinopyroxene and orthopyroxene (001) maxima (Figures 2b–2d). The abundances of plagioclase, clinopyroxene, and orthopyroxene in the studied specimen are 75%, 15%, and 9%, respectively. Therefore, these LPO maxima represent the mineral elongation lineation direction of the silicate fabric and are sub-parallel to the maximum principal axis of the AMS ellipsoid at the site (Figure 2a). The ~18° eastward-dip of the (010) maxima for both the pyroxenes and the plagioclase grains suggest that the silicate fabric preserves ~70° westward dipping ~N-S foliation. Interestingly, these poles to the foliation planes subparallel the intermediate axes of the AMS. In a "normal" situation, the pole to the foliation plane should follow the minima AMS axis direction, as seen in the gabbros from the Oman ophiolite [*Yaouancq and MacLeod*, 2000], suggesting that AMS in these rocks may represent an "Intermediate Fabric". *Rochette et al.* [1992] showed that mixing distributions of single domain to pseudo single domain titanomagnetite grain sizes can result in the Intermediate Fabric where K_2 and K_3 susceptibility axes may interchange their directions, leading to a non unique presentation of the silicate fabric by the AMS tensors. Indeed, remanence magnetization in the Troodos gabbros is carried by single to pseudo single domain titanomagnetite grain sizes [*Granot et al.*, 2006, 2007], and we therefore use only K_1 susceptibility data. We find a spatial coherence of K_1 directions for adjacent sites (Figure 1), distributed over a 10 km scale region, and hence presume that the measured K_1 directions mimic the large-scale lineation pattern of the silicate fabric. We conclude that the close similarity between the lineation patterns of the silicate and magnetic fabrics (i.e., EBSD vs. AMS), and the lack of solid-state deformation [*Abelson et al.*, 2001] indicate that the preferred directions of AMS principal axes most likely represent the last stages of magma flow directions, before the solidification of the magma.

5. Discussion

[11] Tectonic rotations associated with seafloor spreading are known to have affected all crustal levels of the Troodos igneous basement, and must be corrected for in order to recover the original orientation of the petrofabrics within the sampled gabbros [*Granot et al.*, 2006]. Paleomagnetic studies of the upper crust and overlying sedimentary sequence [e.g., *Morris et al.*, 2006] showed that the entire ophiolite had rotated by nearly 90° anti-clockwise during the emplacement (late Cretaceous to early Eocene), leading to an expected remanent magnetization direction of 273°/38° (α_{95} = 6.5°). Any deviation of remanent magnetization from this direction reflects pre-emplacement accretion-related rotations [e.g., *Allerton and Vine*, 1987; *Bonhommet et al.*, 1988; *Ebert et al.*, 2010; *MacLeod et al.*, 1990]. Although the gabbros studied here lack independent structural information, remanence directions together with the assumed N-S trend of rotation axis (parallels the Solea axis) are sufficient to correct for tectonic rotations. *Granot et al.* [2006] have shown that small rotations of 21° around a rotation axis plunging 7° to the north have been accommodated within the center of the Solea axis. Progressively increasing clockwise rotations eastward indicates that the lower crust in the inside corner has undergone rotations of 44° around a rotation axis plunging 53° to the north (Figure S1). Backstripping these rotations from the magnetic fabric data provides the best estimate of the original orientations of the AMS principal axes, as shown in Figure 1b and auxiliary material.

[12] The spatial distribution of the restored K_1 directions reveals two provinces, each of which has remarkably consistent directions (Figure 1b). These directions represent coherent magma flow patterns and are particularly surprising given the typical discrete magma chamber sizes (10–100 m [*Malpas*, 1990]) that prevailed in the lower Troodos crust. The western province displays near vertical K_1 directions while the eastern province reveals shallow N-S directions. Large offset normal faulting with rotated blocks at the Solea graben and hydrothermal massive sulfide bodies suggest that spreading rate was slow to intermediate (full spreading rate of 20 to 75 mm/yr [*Hurst et al.*, 1994; *Small*, 1998; *Varga et al.*, 1999]). Assuming this range of spreading rates, these 10 to 15 km wide provinces of nearly uniform magma flow (Figure 1) represent minimal time intervals of 0.3 to 1 Myr. The narrow transition zone (<1 km) between the two magmatic provinces corresponds to a maximum accretion time of 0.02 to 0.1 Myr, suggesting that the change in the direction of magma flow was rather abrupt. The subhorizontal N-S magma flow directions, consistent with accretion along the N-S Solea axis (Figure 1), validate our structural reconstruction scheme. Along-axis lateral magma flows near the segment-edge were most likely supplied from the north, i.e. from the segment midpoint towards the transform (Figure 3a).

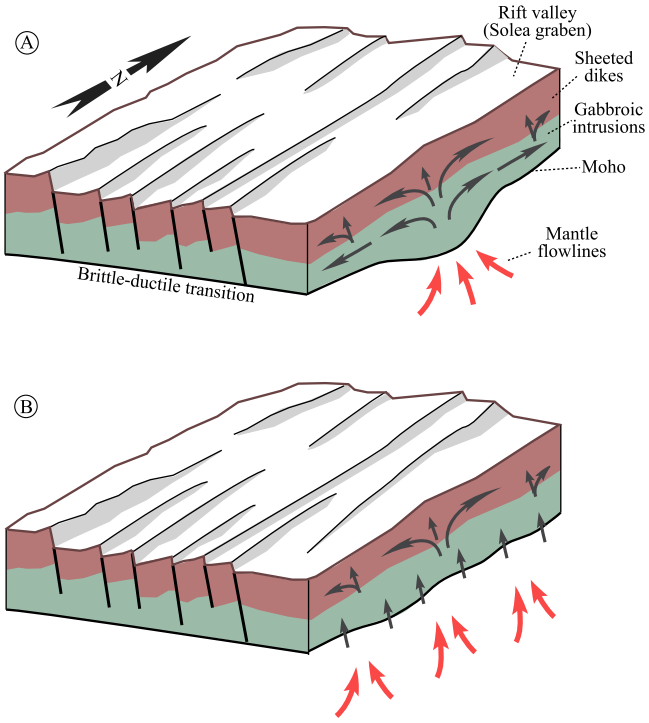


Figure 3. Schematic diagrams illustrating lower crustal magma flow patterns beneath the Troodos spreading center (Solea graben). (a) 3D mantle upwelling and focused melt supply from the mantle abruptly evolved to (b) a period with axially uniform mantle upwelling and melt supply. These diagrams are constrained by data located in the southern-edge of the Solea spreading segment.

These magma flow directions might have corresponded to a period when mantle upwelling was focused at, or near, the center of the Solea segment (Figures 1d and 3a). Vertical magma flows at the segment-edge probably resulted from the emplacement of magma bodies directly underneath the end of the spreading segment and hence correspond to a period when mantle upwelling might have been associated with segment-scale melting conditions (Figure 3b). Previous studies [*Staudigel et al.*, 1999; *Varga et al.*, 1998] showed that horizontal and vertical intrusive directions best describe the propagation of sheeted dikes of the Troodos ophiolite. They argued that these directions reflect the location of the sheeted dikes relative to the feeding magma chamber. By the same token, gabbro flow directions within magma chambers reflect their position relative to where mantle upwelling and melting take place.

[13] The directional transition of the flow between the two magmatic provinces is spatially coincident with the boundary between the rift valley (Solea graben) and the inside corner (Figure 1). This correlation might result from incorrect reconstruction of tectonic rotations, from the late doming of the ophiolite that was centered over the serpentinized mantle (Figure 1), or alternatively, it reflects a casual coincidence. Our tectonic corrections were smaller than 44° and cannot account for the much larger difference in K_1 directions between the two provinces. Late doming of the ophiolite would result in a systematic pattern of rotations. Based on remanence directions (Figure S1), we find this scenario unlikely. We therefore believe the spatial correlation between magma flow provinces and tectonic domains to be casual.

[14] Seismic reflection studies from the Mid-Atlantic Ridge showed that episodic upwelling of mantle material fluctuated with typical periodicities of 0.4 to 0.8 Myr, separated by transition periods as short as ~0.1 Myr [*Canales et al.*, 2000]. These and similar changes in mantle upwelling activity have been suggested to get distributed mainly within the lower crust [*Dunn et al.*, 2005; *Tolstoy et al.*, 1993]. The lower Troodos crust studied here might have recorded one such transition between periods of focused versus axially uniform mantle upwelling and melt supply. Furthermore, our study provides the first direct confirmation for the dominant role of the lower crust in accommodating fluctuations in mantle upwelling and therefore serves as an important modulator of the thermal state along spreading centers.

[15] **Acknowledgments.** This study results from the Master thesis of R.G. at the Hebrew University of Jerusalem and benefited from discussions with Jeff Gee, Mike Cheadle, and Lisa Tauxe. We thank Antony Morris and an anonymous reviewer for their constructive reviews. IPGP contribution number 3210.

[16] The Editor thanks Antony Morris and an anonymous reviewer for their assistance in evaluating this paper.

References

Abelson, M., and A. Agnon (2001), Hotspot activity and plume pulses recorded by geometry of spreading axes, *Earth Planet. Sci. Lett.*, *189*(1–2), 31–47, doi:10.1016/S0012-821X(01)00331-4.

Abelson, M., G. Baer, and A. Agnon (2001), Evidence from gabbro of the Troodos ophiolite for lateral magma transport along a slow-spreading mid-ocean ridge, *Nature*, *409*(6816), 72–75, doi:10.1038/35051058.

Abelson, M., G. Baer, and A. Agnon (2002), Fossil ridge-transform intersection in the Troodos ophiolite: New perspectives from rock magnetism in the gabbro suite and fracture mechanics analysis, *Geochem. Geophys. Geosyst.*, *3*(8), 1046, doi:10.1029/2001GC000245.

Allerton, S. (1989), Fault block rotations in ophiolites: Results of palaeomagnetic studies in the Troodos Complex, in *Paleomagnetic Rotations and Continental Deformation*, *NATO ASI Ser., Ser. C*, vol. 254, edited by C. Kissel and C. Laj, pp. 393–410, Kluwer Acad., Dordrecht, Netherlands.

Allerton, S., and F. Vine (1987), Spreading structure of the Troodos ophiolite, Cyprus: Some paleomagnetic constraints, *Geology*, *15*, 593–597, doi:10.1130/0091-7613(1987)15<593:SSOTTO>2.0.CO;2.

Bonatti, E., M. Ligi, D. Brunelli, A. Cipriani, P. Fabretti, V. Ferrante, L. Gasperini, and L. Ottolini (2003), Mantle thermal pulses below the Mid-Atlantic Ridge and temporal variations in the formation of oceanic lithosphere, *Nature*, *423*(6939), 499–505, doi:10.1038/nature01594.

Bonhommet, N., P. Roperch, and F. Calza (1988), Paleomagnetic arguments for block rotations along the Arakapas fault (Cyprus), *Geology*, *16*, 422–425, doi:10.1130/0091-7613(1988)016<0422:PAFBRA>2.3.CO;2.

Canales, J., J. Collins, J. Escartín, and R. Detrick (2000), Seismic structure across the rift valley of the Mid-Atlantic Ridge at 23°20′ (MARK area): Implications for crustal accretion processes at slow spreading ridges, *J. Geophys. Res.*, *105*(B12), 28,411–28,425, doi:10.1029/2000JB900301.

Constable, C., and L. Tauxe (1990), The bootstrap for magnetic susceptibility tensors, *J. Geophys. Res.*, *95*(B6), 8383–8395, doi:10.1029/JB095iB06p08383.

Dunn, R. A., V. Lekic, R. S. Detrick, and D. R. Toomey (2005), Three-dimensional seismic structure of the Mid-Atlantic Ridge (35°N): Evidence for focused melt supply and lower crustal dike injection, *J. Geophys. Res.*, *110*, B09101, doi:10.1029/2004JB003473.

Ebert, Y., R. Kessel, R. Shaar, A. Agnon, and H. Ron (2010), Petrology and rock magnetism of the gabbro of Troodos ophiolite, *Phys. Earth Planet. Inter.*, *183*, 413–420, doi:10.1016/j.pepi.2010.09.006.

Gee, J., W. Meurer, P. Selkin, and M. Cheadle (2004), Quantifying three-dimensional silicate fabrics in cumulates using cumulative distribution functions, *J. Petrol.*, *45*(10), 1983–2009, doi:10.1093/petrology/egh045.

Granot, R., M. Abelson, H. Ron, and A. Agnon (2006), The oceanic crust in 3D: Paleomagnetic reconstruction in the Troodos ophiolite gabbro, *Earth Planet. Sci. Lett.*, *251*(3–4), 280–292, doi:10.1016/j.epsl.2006.09.019.

Granot, R., L. Tauxe, J. S. Gee, and H. Ron (2007), A view into the Cretaceous geomagnetic field from analysis of gabbros and submarine

glasses, *Earth Planet. Sci. Lett.*, *256*(1–2), 1–11, doi:10.1016/j.epsl.2006.12.028.

Hargraves, R., D. Johnson, and C. Chan (1991), Distribution anisotropy: The cause of AMS in igneous rocks?, *Geophys. Res. Lett.*, *18*(12), 2193–2196, doi:10.1029/91GL01777.

Hosford, A., J. Lin, and R. S. Detrick (2001), Crustal evolution over the last 2 m.y. at the Mid-Atlantic Ridge OH-1 segment, 35°N, *J. Geophys. Res.*, *106*(B7), 13,269–13,285, doi:10.1029/2001JB000235.

Hurst, S. D., E. M. Moores, and R. Varga (1994), Structural and geophysical expression of the Solea graben, Troodos ophiolite, Cyprus, *Tectonics*, *13*(1), 139–156, doi:10.1029/93TC02066.

Jelinek, V. (1981), Characterization of the magnetic fabric of rocks, *Tectonophysics*, *79*, 63–67, doi:10.1016/0040-1951(81)90110-4.

Kent, G. M., A. J. Harding, and J. A. Orcutt (1993), Distribution of magma beneath the East Pacific Rise between the Clipperton Transform and the 9°17′N Deval from forward modeling of common depth point data, *J. Geophys. Res.*, *98*(B8), 13,945–13,969, doi:10.1029/93JB00705.

MacLeod, C. J., S. Allerton, I. G. Gass, and C. Xenophontos (1990), Structure of a fossil ridge-transform intersection in the Troodos ophiolite, *Nature*, *348*, 717–720, doi:10.1038/348717a0.

MacLeod, C., F. Boudier, G. Yaouancq, and C. Richter (1996), Gabbro fabrics from Site 894, Hess Deep: Implications for magma chamber processes at the East Pacific Rise, *Proc. Ocean Drill. Prog. Results*, *147*, 317–328.

Magde, L. S., A. H. Barclay, D. R. Toomey, R. S. Detrick, and J. A. Collins (2000), Crustal magma plumbing within a segment of the Mid-Atlantic Ridge, 35°N, *Earth Planet. Sci. Lett.*, *175*(1–2), 55–67, doi:10.1016/S0012-821X(99)00281-2.

Malpas, J. (1990), Crustal accretionary processes in the Troodos ophiolite, Cyprus: Evidence from field mapping and deep crustal drilling, in *Proceedings of the Symposium "TROODOS 1987" on Ophiolites and Oceanic Crustal Analogues*, edited by J. Malpas et al., pp. 65–74, Geol. Surv. Dep., Nicosia.

Morris, A., K. M. Creer, and A. H. F. Robertson (1990), Palaeomagnetic evidence for clockwise rotations related to dextral shear along the Southern Troodos Transform Fault, Cyprus, *Earth Planet. Sci. Lett.*, *99*(3), 250–262, doi:10.1016/0012-821X(90)90114-D.

Morris, A., M. W. Anderson, J. Inwood, and A. H. F. Robertson (2006), Palaeomagnetic insights into the evolution of Neotethyan oceanic crust in the eastern Mediterranean, in *Tectonic Development of the Eastern Mediterranean Region*, edited by A. H. F. Robertson and D. Mountrakis, *Geol. Soc. Spec. Publ.*, *260*, 351–372, doi:10.1144/GSL.SP.2006.260.01.15.

Mukasa, S. B., and J. N. Ludden (1987), Uranium-Lead isotopic ages of plagiogranites from the Troodos ophiolite, Cyprus, and their tectonic significance, *Geology*, *15*(9), 825–828, doi:10.1130/0091-7613(1987)15<825:UIAOPF>2.0.CO;2.

Muller, M. R., T. A. Minshull, and R. S. White (1999), Segmentation and melt supply at the Southwest Indian Ridge, *Geology*, *27*(10), 867–870, doi:10.1130/0091-7613(1999)027<0867:SAMSAT>2.3.CO;2.

Olive, J., M. Behn, and B. Tucholke (2010), The structure of oceanic core complexes controlled by the depth distribution of magma emplacement, *Nat. Geosci.*, *3*(7), 491–495, doi:10.1038/ngeo888.

Perfit, M., D. Fornari, M. Smith, and J. Bender (1994), Small-scale spatial and temporal variations in mid-ocean ridge crest magmatic processes, *Geology*, *22*(4), 375–379, doi:10.1130/0091-7613(1994)022<0375:SSSATV>2.3.CO;2.

Robertson, A., and C. Xenophontos (1993), Development of concepts concerning the Troodos ophiolite and adjacent units in Cyprus, in *Magmatic Processes and Plate Tectonics*, edited by H. M. Prichard et al., *Geol. Soc. Spec. Publ.*, *76*, 85–119, doi:10.1144/GSL.SP.1993.076.01.05.

Rochette, P., M. Jackson, and C. Aubourg (1992), Rock magnetism and the interpretation of anisotropy of magnetic susceptibility, *Rev. Geophys.*, *30*(3), 209–226, doi:10.1029/92RG00733.

Rubin, K. H., J. M. Sinton, J. Maclennan, and E. Hellebrand (2009), Magmatic filtering of mantle compositions at mid-ocean-ridge volcanoes, *Nat. Geosci.*, *2*(5), 321–328, doi:10.1038/ngeo504.

Schouten, H., and P. B. Kelemen (2002), Melt viscosity, temperature and transport processes, Troodos ophiolite, Cyprus, *Earth Planet. Sci. Lett.*, *201*(2), 337–352, doi:10.1016/S0012-821X(02)00709-4.

Searle, R. C., and J. Escartin (2004), The rheology and morphology of oceanic lithosphere and mid-ocean ridges, in *Mid-Ocean Ridges: Hydrothermal Interactions Between the Lithosphere and the Oceans*, *Geophys. Monogr. Ser.*, vol. 148, edited by C. German et al., pp. 63–94, AGU, Washington, D. C.

Small, C. (1998), Global systematics of mid-ocean ridge morphology, in *Faulting and Magmatism at Mid-Ocean Ridges*, *Geophys. Monogr. Ser.*, vol. 106, edited by R. W. Buck et al., pp. 1–26, AGU, Washington, D. C.

Staudigel, H., et al. (1999), Geochemistry and intrusive directions in sheeted dikes in the Troodos ophiolite: Implications for mid-ocean ridge spreading centers, *Geochem. Geophys. Geosyst.*, *1*(1), 1001, doi:10.1029/1999GC000001.

Tauxe, L., J. S. Gee, and H. Staudigel (1998), Flow directions in dikes from anisotropy of magnetic susceptibility data: The bootstrap way, *J. Geophys. Res.*, *103*(B8), 17,775–17,790, doi:10.1029/98JB01077.

Tolstoy, M., A. J. Harding, and J. A. Orcutt (1993), Crustal thickness on the Mid-Atlantic Ridge: Bull's-eye gravity anomalies and focused accretion, *Science*, *262*(5134), 726–729, doi:10.1126/science.262.5134.726.

Toomey, D. R., D. Jousselin, R. A. Dunn, W. S. D. Wilcock, and R. S. Detrick (2007), Skew of mantle upwelling beneath the East Pacific Rise governs segmentation, *Nature*, *446*(7134), 409–414, doi:10.1038/nature05679.

Tucholke, B. E., and J. Lin (1994), A geological model for the structure of ridge segments in slow-spreading ocean crust, *J. Geophys. Res.*, *99*(B6), 11,937–11,958, doi:10.1029/94JB00338.

Tucholke, B. E., J. Lin, M. C. Kleinrock, M. A. Tivey, T. B. Reed, J. Goff, and G. E. Jaroslow (1997), Segmentation and crustal structure of the western Mid-Atlantic Ridge flank, 25°25′–27°10′N and 0–29 m.y., *J. Geophys. Res.*, *102*(B5), 10,203–10,223, doi:10.1029/96JB03896.

Varga, R. J., J. S. Gee, H. Staudigel, and L. Tauxe (1998), Dike surface lineations as magma flow indicators within the sheeted dike complex of the Troodos ophiolite, Cyprus, *J. Geophys. Res.*, *103*(B3), 5,241–5,256, doi:10.1029/97JB02717.

Varga, R. J., J. S. Gee, L. Bettison-Varga, R. S. Anderson, and C. L. Johnson (1999), Early establishment of seafloor hydrothermal systems during structural extension: paleomagnetic evidence from the Troodos ophiolite, Cyprus, *Earth Planet. Sci. Lett.*, *171*, 221–235, doi:10.1016/S0012-821X(99)00147-8.

Yaouancq, G., and C. J. MacLeod (2000), Petrofabric investigation of gabbros from the Oman ophiolite: Comparison between AMS and rock fabric, *Mar. Geophys. Res.*, *21*, 289–306, doi:10.1023/A:1026774111021.

M. Abelson, Geological Survey of Israel, 30 Malkhe Israel St., Jerusalem 95501, Israel.

A. Agnon and H. Ron, Institute of Earth Sciences, Hebrew University of Jerusalem, Jerusalem 91904, Israel.

R. Granot, Department of Geological and Environmental Sciences, Ben-Gurion University of the Negev, Beer-Sheva 84105, Israel. (rgranot@bgu.ac.il)

M. W. Lusk, Department of Geology and Geophysics, University of Wyoming, Laramie, WY 82701, USA.